Infection and Immunity

Systemic Macrophage Depletion Inhibits Helicobacter bilis-Induced Proinflammatory Cytokine-Mediated Typhlocolitis and Impairs Bacterial Colonization Dynamics in a BALB/c *Rag2*$^{-/-}$ Mouse Model of Inflammatory Bowel Disease

Sureshkumar Muthupalani, Zhongming Ge, Yan Feng, Barry Rickman, Melissa Mobley, Amanda McCabe, Nico Van Rooijen and James G. Fox

Infect. Immun. **2012, 80(12):4388. DOI: 10.1128/IAI.00530-12. Published Ahead of Print 1 October 2012.**

IAI Journals.ASM.org

Systemic Macrophage Depletion Inhibits *Helicobacter bilis*-Induced Proinflammatory Cytokine-Mediated Typhlocolitis and Impairs Bacterial Colonization Dynamics in a BALB/c *Rag2*$^{-/-}$ Mouse Model of Inflammatory Bowel Disease

Sureshkumar Muthupalani,[a] Zhongming Ge,[a] Yan Feng,[a] Barry Rickman,[a] Melissa Mobley,[a] Amanda McCabe,[a] Nico Van Rooijen,[b] and James G. Fox[a,c]

Division of Comparative Medicine[a] and Department of Biological Engineering,[c] Massachusetts Institute of Technology, Cambridge, Massachusetts, USA, and Department of Molecular Cell Biology, Vrije Universiteit Medical Center, Amsterdam, Netherlands[b]

Helicobacter bilis*, an enterohepatic helicobacter, is associated with chronic hepatitis in aged immunocompetent inbred mice and inflammatory bowel disease (IBD) in immunodeficient mice. To evaluate the role of macrophages in *H. bilis*-induced IBD, *Rag2*$^{-/-}$ BALB/c or wild-type (WT) BALB/c mice were either sham dosed or infected with *H. bilis* Missouri strain under specific-pathogen-free conditions, followed by an intravenous injection of a 0.2-ml suspension of liposomes coated with either phosphate-buffered saline (control) or clodronate (a macrophage depleting drug) at 15 weeks postinfection (wpi). At 16 wpi, the ceca of *H. bilis*-infected *Rag2*$^{-/-}$ mice treated with control liposomes had significantly higher histopathological lesional scores (for cumulative typhlitis index, inflammation, edema, epithelial defects, and hyperplasia) and higher counts of F4/80^{+} macrophages and MPO^{+} neutrophils compared to *H. bilis*-infected *Rag2*$^{-/-}$ mice treated with clodronate liposomes. In addition, cecal quantitative PCR analyses revealed a significant suppression in the expression of macrophage-related cytokine genes, namely, *Tnfa*, *Il-1β*, *Il-10*, *Cxcl1*, and *iNos*, in the clodronate-treated *H. bilis*-infected *Rag2*$^{-/-}$ mice compared to the *H. bilis*-infected *Rag2*$^{-/-}$ control mice. Finally, cecal quantitative PCR analyses also revealed a significant reduction in bacterial colonization in the clodronate-treated *Rag2*$^{-/-}$ mice. Taken together, our results suggest that macrophages are critical inflammatory cellular mediators for promoting *H. bilis*-induced typhlocolitis in mice.

Inflammatory bowel disease (IBD) constitutes spectra of chronic, idiopathic, and relapsing complex multifactorial inflammatory disorders of the gastrointestinal tract in humans with two well-recognized clinicopathological manifestations, namely, ulcerative colitis and Crohn's disease. Both of these conditions are associated with an increased risk of developing colitis associated colorectal cancers (21, 42, 38, 53). Various mouse models to study IBD include spontaneous colitis models, chemically induced colitis models, adoptive cell transfer models, colitis in immunodeficient mice, or genetically engineered models or any combination of these models (8, 12, 22, 29, 32, 35, 50, 51). Epidemiological data and animal models of IBD implicate a dynamic interplay of multiple factors, including genetic susceptibility, intestinal microbiota, host innate and adaptive immune components, and environmental effects in the pathogenesis of IBD and colitis-associated carcinogenesis (1, 4, 7, 12, 22, 38, 53).

Commensal gut microbiota are key players in the development and maintenance of the host gastrointestinal immune homeostasis and in the initiation of IBD following enteric mucosal damage observed with infections, chemicals such as dextran sodium sulfate (DSS), drug toxicities, radiation therapy, and antibiotic therapy (1, 22, 32, 37). Among the gut microflora are members of the enterohepatic *Helicobacter* species (EHS) that are prevalent in mice housed in academic facilities (44, 45, 46, 47). Of these, *Helicobacter hepaticus* is the best studied in terms of its ability to cause murine strain-dependent hepatitis and IBD, as well hepatic and colon cancers in *Il-10*$^{-/-}$ mice, *SCID* mice (lacks T and B cells), and *Rag2*$^{-/-}$ mice (lacks functional lymphocytes) (12). *H. bilis* is another Gram-negative, microaerophilic EHS that was first isolated from the livers and intestines of aged inbred strains of mice with hepatitis (15) and subsequently from the livers of outbred mice (13). *H. bilis* causes typhlocolitis and/or cholangiohepatitis in a variety of immunocompromised mice, including *SCID*, *Il-10*$^{-/-}$, *Mdr1a*$^{-/-}$, and *TCRα*$^{-/-}$ mice (12, 29, 45). *H. bilis* or *H. hepaticus* infection in 129-Smad3tm/Par/J (referred to as *Smad3*$^{-/-}$) mice leads to the development of colitis-associated mucinous colonic adenocarcinoma that is strongly correlated with the expression of *Il-1b*, *Mip-1a*, and *Cd5* (RANTES) (9). *H. bilis* is also associated with proliferative typhlocolitis, chronic hepatitis, hepatic dysplasia, and biliary hyperplasia in aged Syrian hamsters (14), as well as IBD/colitis in athymic nude rats (20). Further, *H. bilis* has been incriminated to play a role in human cholecystitis and gallbladder cancer from studies in Japan, Thailand, and Chile (11, 24, 34). In immunocompetent mice (C3H) mice with defined microbiota, *H. bilis* infection—even in the absence of overt colitis—results in a significant increase in the expression pattern of a plethora of mucosal genes, including those

Received 18 May 2012 Returned for modification 24 June 2012
Accepted 23 September 2012
Published ahead of print 1 October 2012
Address correspondence to Sureshkumar Muthupalani, smuthu01@mit.edu, or James G. Fox, jgfox@mit.edu.
Editor: J. B. Bliska

doi:10.1128/IAI.00530-12

involved in lymphocyte activation (e.g., *Cd28* and *Tnfsf13b*) and regulation (e.g., *Il-17a*) and in inflammatory cell chemotaxis (e.g., *Itgb2*, *Ccl8*, and *Ccr5*) (27). Importantly, *H. bilis* can cause the exacerbation of DSS-induced colitis, as shown in a study using C3H/HeN:TAC mice colonized with defined microflora (28). Recent studies in our laboratory performed in C57BL/6 mice have highlighted the role of EHS, *H. bilis*, *H. muridarum*, and *H. hepaticus* in immunomodulating the pathogenesis of *H. pylori* via a Th17 regulatory pathway (18, 26).

Specialized gut-resident dendritic cells (DCs) and macrophages display remarkable plasticity and partial overlap in their functionality, phenotypes, and expression of various cellular markers, such as Cd11b (macrophages, both positive and negative DCs), Cd11c (DCs chiefly, some macrophage subsets), Cd103 (both positive and negative DCs), Cd8α, Cd45, and F4/80 (macrophages chiefly, some DC subsets), depending upon their location and individual subset population (5, 10, 19, 37, 40). Both macrophages and DCs are key players in the immune defense against both commensal and pathogens and are modulators of the regulatory T cell population (5, 10, 19, 40). In IBD, macrophages within the inflamed mucosa are derived from mainly circulating macrophages and, upon stimulation, secrete various proinflammatory cytokines, such as interleukin-1 (IL-1), IL-6, IL-8, IL-12, IL-18, and tumor necrosis factor alpha (TNF-α), all of which can mediate the associated pathology (41, 53). Macrophages and other phagocytes, primarily DCs and neutrophils, mediate the release of reactive oxygen species, including myeloperoxidase (MPO) (predominantly from neutrophils) and nitric oxide (from macrophages), with purported direct epithelial injury and a battery of subcellular and molecular damage to DNA, RNA, protein, lipids, and metabolites in IBD and colon cancer in humans and animal models (2, 7, 21, 28, 33, 48).

Selective macrophage depletion, by means of the macrophage suicide technique utilizing liposome-mediated intracellular delivery of dichloromethylene-biphosphonate (Cl_2MBP [clodronate]) is a well-established experimental protocol that is routinely used to address the contribution of innate immune cells in the pathogenesis of inflammatory disorders (35, 36, 49, 50). Depending upon the route of administration, the liposomes containing clodronate are rapidly engulfed by professional phagocytes, chiefly macrophages and certain subsets of DCs, in various tissues, leading to the formation of an endosome (49, 52). The next set of events in the ingested macrophages include the fusion of the endosome with the phagosome, resulting in the formation of a phagolysosome with low pH, followed by the activation of phospholipases, leading to the degradation of phagolysosomal membranes and the release of free clodronate into the cytosol (49, 52). Free clodronate is a negatively charged, readily diffusible, water-soluble biphosphonate that chemically mimics cellular pyrophosphates and is acted upon by several class II aminoacyl-tRNA synthetases to produce a nonhydrolyzable ATP analog, namely, adenosine 5′-(β,γ-dichloromethylene)triphosphate (AppCCl_2p) (25, 49, 52). AppCCl_2p is toxic to cells and is presumed to cross the outer mitochondrial membrane leaflets and irreversibly binds to and inactivates ATP/ADP translocases on the inner membrane, leading to membrane pore formation, loss of mitochondrial membrane integrity, mitochondrial depolarization, and caspase-mediated apoptotic cell death (25). Systemically administered clodronate in encapsulated liposome form is rapidly cleared from the blood within hours by means of uptake by different subtypes of macrophages in the liver, spleen, lymph nodes, gut, lungs, and other organs. Clodronate-mediated macrophage apoptotic cellular debris is usually seen only during the first 2 days posttreatment, and hence *in vivo* experimental analyses are usually performed 2 or more days after clodronate treatment (49, 52).

Various experimental studies have successfully used the clodronate liposome-mediated strategy as a tool to study the role of macrophages in different settings of IBD (35, 36, 50, 52). These include the systemic depletion of macrophages and DCs, as well as local depletion of these cells by rectal administration in different settings of DSS colitis in various immunodeficient murine strains. Specifically, studies of IL-10 knockout (KO) mice, SHIP$^{-/-}$ mice (i.e., deficient in the hematopoiesis-specific negative regulator of the phosphatidylinositol 3-kinase pathway, skewed macrophage [M2a] phenotype), and CD11c-DTR transgenic mice (i.e., deficient in DCs) have highlighted the importance of these cells in the pathogenesis of IBD (30, 35, 36, 50, 51, 52).

In the present study, we evaluated the effect of systemic depletion of macrophages via administration of clodronate in an encapsulated liposome form in a *Rag2*$^{-/-}$ murine model of *H. bilis*-induced typhlocolitis. The impact of macrophage depletion was assessed in terms of *H. bilis*-induced overall typhlocolitis, intestinal tissue cytokine profiles, and *H. bilis* colonization dynamics.

MATERIALS AND METHODS

Bacterial culture, DNA preparation, and quantitative PCR for *H. bilis*. *H. bilis* Missouri strain was cultured under microaerobic conditions (80% N_2, 10% H_2, 10% CO_2) at 37°C on Columbia blood agar plates (Remel Laboratories) for 3 to 4 days. For experimental inoculation, the bacterial density was adjusted to ~10^9 per ml in phosphate-buffered saline (PBS) on the basis of an optical density at 600 nm of 1. Mice were orally gavaged with 0.2 ml (~2×10^8 organisms) of an *H. bilis* suspension every other day for three doses. The DNA was extracted from the cultured *H. bilis* and from cecal tissues by use of a High-Pure PCR template preparation kit (Roche Molecular Biochemicals, Indianapolis, IN). Cecal levels of *H. bilis* were measured and normalized in reference to mouse DNA using quantitative PCR as previously described (26).

***In vivo H. bilis* infection and macrophage depletion.** Wild-type (WT) BALB/c mice or *Rag2*$^{-/-}$ BALB/c mice obtained from Taconic Farms (Germantown, NY) were housed in groups of five in polycarbonate microisolator cages on hardwood bedding (PharmaServ, Framingham, MA) under specific-pathogen-free conditions (free of *Helicobacter* spp., *Citrobacter rodentium*, *Salmonella* spp., endoparasites, ectoparasites, and exogenous murine viral pathogens). All animals were housed in an Association for Assessment and Accreditation of Laboratory Animal Care (AAALAC) International-accredited facility, and all animal experimental protocols approved by the MIT Committee on Animal Care. Mice were maintained at standard conditions of 70 ± 2°F in 30 to 70% relative humidity with a 12-h/12-h light/dark cycle, were fed standard rodent chow (Purina Mills, St. Louis, MO), and were provided with water *ad libitum*. A total of 52 animals were used in the study, and these animals were divided among various treatment groups as outlined in Table 1. These were divided into animals infected with *H. bilis* as described above or uninfected animals with either WT or *Rag2*$^{-/-}$ backgrounds. Infected mice or sham-dosed mice were maintained for 14 to 16 weeks postinfection (wpi) under specific-pathogen-free conditions prior to euthanasia and postmortem examination. A subset of mice from both WT and *Rag2*$^{-/-}$ backgrounds at exactly 7 days prior to their euthanasia were administered intravenously via tail vein a suspension of 0.2 ml containing either clodronate-encapsulated liposomes (active form) or PBS-coated liposomes (inactive form) to serve as a control. Clodronate (Roche Diag-

TABLE 1 Experimental mice, *H. bilis* infection status, and treatments

Mouse strain	Uninfected mice		*H. bilis*-infected mice	
	Treatment	No. of animals	Treatment	No. of animals
BALB/c WT	Clodronate liposomes	5	Clodronate liposomes	2
	Control (PBS) liposomes	5	Control (PBS) liposomes	4
BALB/c *Rag2*$^{-/-}$	Clodronate liposomes	5	Clodronate liposomes	13 (9 M, 4 F)
	Control (PBS) liposomes	5	Control (PBS) liposomes	13 (9 M, 4 F)

nostics GmbH, Mannheim, Germany) at a concentration of 0.25 g/ml of PBS was encapsulated in liposomes according to an established protocol as described previously (49, 52).

Necropsy and histopathology. At necropsy, a complete gross examination of abdominal and thoracic organs was performed. Representative samples of feces, stomachs, ceca, colons, livers, and gallbladders were collected in freeze medium for culture and/or PCR, and the tissues were fixed in 10% neutral buffered formalin for routine histological processing. Hematoxylin-eosin (H&E)-stained sections of the cecum, including the junctions of the cecum, ileum, and proximal colon, colon (proximal, transverse, and distal colon), and liver were evaluated by two board-certified comparative pathologists (B. Rickman and S. Muthupalani), who were blinded to sample identity as described previously (39). Briefly, the intestinal sections were scored on a scale of 0 to 4 for inflammation, epithelial defects, crypt atrophy, hyperplasia, and dysplasia/neoplasia, and the cumulative scores were represented as either the colitis index or the typhlitis index. Liver sections were examined in on a scale of 0 to 4 for inflammation.

Immunohistochemistry. Using previously established protocols, we evaluated macrophages, neutrophils, and DCs in intestinal tissue sections by avidin-biotin complex immunohistochemistry with antibodies specific for MPO (1:75; RB-373-A [Thermo Scientific]), a predominantly neutrophil-specific marker; F4/80 (1:150; MF48015 [Caltag Laboratories]), a macrophage-specific marker; and S100 (1:40; AbD Serotec, Inc.), a neuroglial marker that also identifies DC subsets) (43). Briefly, ileocecal and colonic sections from 10 randomly selected animals (five males and five females) per group for each different time point were analyzed. Five randomly selected, full-thickness mucosal segments at a ×40 objective field magnification per mouse were screened to quantify the total number immunopositive cells in the mucosa and submucosa. The data were analyzed using unpaired Student *t* test, and the values were plotted as the average number of positive cells/×40 high-power objective field (HPF).

Tissue cytokines. To correlate the histopathological lesion severity with the inflammatory molecular markers, we analyzed cytokine gene expression levels in the cecum. One-centimeter segments of cecum near the junction were harvested immediately after mice were euthanized, and the segments were snap-frozen in liquid nitrogen. The total RNA from cecal samples were prepared using TRIzol reagents by following the manufacturer's instructions (Invitrogen, Carlsbad, CA). cDNA from cecal mRNA (2 μg) was reverse transcribed by using a High-Capacity cDNA archive kit (Applied Biosystems, Foster City, CA) according to the supplier's instructions. The transcript levels of IL-1β, TNF-α, IL-10, Cox2, iNOS, and Cxcl1 in individual samples of the cecum were measured by quantitative PCR using TaqMan gene expression assays in the ABI Prism sequence detection system 7500 Fast (Applied Biosystems). Cecal RNA from all individual mice from the various infected and uninfected groups (both WT and *Rag2*$^{-/-}$ mice) with or without clodronate treatment was used for individual cytokine analyses. WT and *Rag2*$^{-/-}$ mice were compared separately for statistical purposes, and the uninfected mice from each genotype served as their respective controls. All target genes were normalized to the endogenous control glyceraldehyde-3-phosphate dehydrogenase (GAPDH) mRNA and expressed as fold changes in reference to sham-dosed control mice using the comparative threshold cycle (C_T) method (Applied Biosystems, *User Bulletin No. 2*).

Statistical analysis. Statistical analyses of nonparametric histopathological scores was performed using the Mann-Whitney U test and are represented as median values with upper and lower quartiles. Immunohistochemical quantitative data between different groups was analyzed using the unpaired Student *t* test and are presented as means ± the standard errors of the mean. The cytokine data were analyzed using a two-tailed Student *t* test. For all analyses, a P value of <0.05 was considered statistically significant. All analyses were performed using Prism software (GraphPad, San Diego, CA).

RESULTS

Systemic macrophage depletion attenuated typhlocolonic inflammation in *H. bilis*-infected *Rag2*$^{-/-}$ mice. In this experiment, the ceca and colons of various experimental animals with differences in genetic background (BALB/c WT or BALB/c *Rag2*$^{-/-}$ mice), infection status (with or without *H. bilis*), and treatment type (control liposomes encapsulated with PBS or liposomes encapsulated with clodronate) were systematically evaluated for the changes in the various histomorphological parameters. As shown in Fig. 1a, the *H. bilis*-infected *Rag2*$^{-/-}$ mice (n = 13) at 16 wpi treated with control (PBS) liposomes (7 days posttreatment) had significantly higher overall typhlitis index scores than *H. bilis*-infected *Rag2*$^{-/-}$ mice (n = 13) (P = 0.002) treated with clodronate-encapsulated liposomes. Although not statistically significant, a similar trend was also observed in the colon with respect to the overall colitis index scores between the two *H. bilis*-infected groups (Fig. 1b). For the cecum, histological lesions were reflected in significantly higher scores for inflammation (P = 0.001), edema (P = 0.015), epithelial defects ($P < 0.0001$), and hyperplasia (P = 0.004) in PBS (placebo) liposome *H. bilis*-infected mice compared to clodronate liposome-treated infected mice (Fig. 2). The degree of typhlitis in the PBS-treated *H. bilis*-infected *Rag2*$^{-/-}$ mice ranged from mild to moderate mixed inflammation composed predominantly of macrophages, neutrophils, and eosinophils (score range, 1 to 2; median, 1; mean, 1.3) with associated mild edema (range, 0 to 2; median, 0; mean, 0.8), mild epithelial defects (range, 0.5 to1; median, 1; mean, 0.9), and mild to moderate hyperplasia (range, 0 to 3; median, 1; mean, 1). In comparison, systemic depletion of macrophages in *H. bilis*-infected *Rag2*$^{-/-}$ mice resulted in no to minimal inflammation (range, 0 to 1; median, 0; mean, 0.3), minimal edema (range, 0 to 1; median, 0; mean, 0.3), minimal epithelial defects (range, 0 to 1; median, 0; mean, 0.2), and no to minimal hyperplasia (range, 0 to 1; median, 0; mean, 0.19). In both of these groups, crypt atrophy and dysplasia were mostly inconsequential, except in one infected PBS-treated mouse that exhibited minimal cecal epithelial dysplasia (Fig. 2 and 3). The trend for higher colonic lesional index scores in control liposome-treated infected mice was reflected by marginally higher scores in the categories of inflammation, epi-

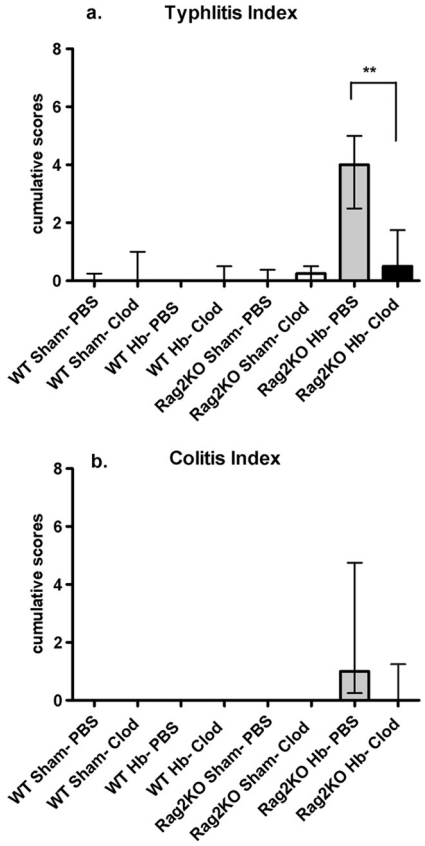

FIG 1 Cecal (a) or colonic (b) tissues of *H. bilis*-infected or uninfected (sham) BALB/c mice of both *Rag2*$^{-/-}$ (Rag2KO) or wild-type (WT) backgrounds treated with either control (PBS) liposomes or clodronate (Clod) were histologically graded at 16 wpi for inflammation, edema, epithelial defects, crypt atrophy, hyperplasia, and dysplasia, and the cumulative scores are represented as typhlitis or colitis index, respectively. Clodronate treatment significantly attenuated *H. bilis*-induced typhlitis in *Rag2*$^{-/-}$ mice, and no significant pathology was observed in both infected and uninfected WT animals. Individual bars represent the median scores with interquartile ranges (*, $P < 0.05$; **, $P < 0.01$; ***, $P < 0.001$).

thelial defects, and hyperplasia compared to clodronate liposome-treated mice (data not shown).

Additional controls for the experiment included uninfected WT (BALB/c) treated with either control (PBS) liposomes ($n = 5$) or clodronate-encapsulated liposomes ($n = 5$) and WT *H. bilis*-infected mice treated with either control (PBS) liposomes ($n = 5$) or clodronate-encapsulated liposomes ($n = 5$), as well as uninfected *Rag2*$^{-/-}$ mice treated with either control liposomes ($n = 4$) or clodronate-encapsulated liposomes ($n = 2$). As expected in these various groups of control mice, the ceca and colons of most animals were normal except for minimal inflammation and/or associated changes in a few, as shown by the cumulative lesion indices in Fig. 1. Also, the livers of *H. bilis*-infected mice did not show any significant inflammation or other pathological alterations.

Clodronate treatment in *H. bilis*-infected *Rag2*$^{-/-}$ mice resulted in a significant reduction in cecal macrophage and neutrophil counts. In addition, by quantitative immunohistochemical analysis, we observed that the clodronate liposome-treated *H. bilis*-infected *Rag2*$^{-/-}$ mice had significantly decreased numbers of F4/80^{+} macrophages colonizing the cecal mucosa than control liposome-treated *H. bilis*-infected *Rag2*$^{-/-}$ mice ($P = 0.004$, $n = 6$ [clodronate versus control]; means ± the standard deviations [SD], 49.5 ± 8 versus 32.3 ± 3.8, per 40× HPF) (Fig. 4). Interestingly, given the importance of macrophages in chemokine production (e.g., Cxcl1) and neutrophil influx during IBD and other inflammatory states (6, 34, 41, 46), the systemic depletion of macrophages in *H. bilis*-infected *Rag2*$^{-/-}$ mice in the present study also resulted in a significant reduction ($P < 0.015$) in cecal neutrophil counts compared to their placebo (PBS) liposome-treated counterparts (Fig. 4). Upon S100 immunostaining, we observed positive staining of DCs (on the basis of morphology) in the mucosae of *H. bilis*-infected animals, and this was decreased in magnitude in clodronate-treated *H. bilis*-infected animals, although some cross-reactivity was also observed in few neutrophils (hence, the data are not presented).

Reduction of intestinal macrophages counts in clodronate-treated *H. bilis*-infected *Rag2*$^{-/-}$ mice is correlated with a significant suppression of macrophage-related inflammatory cytokines. To evaluate the importance of macrophages and related cytokines in this model of *H. bilis*-induced typhlocolitis, the transcript levels of select cytokines and chemokines were measured at 16 wpi by quantitative PCR in the cecal tissues of both *Rag2*$^{-/-}$ mice and WT mice intravenously treated with clodronate. These findings were correlated with histopathological disease severity. In the clodronate-treated *H. bilis*-infected *Rag2*$^{-/-}$ mice, there was a significant suppression in the cecal mRNA levels of the cytokines, expressed predominantly or acted upon by the monocyte/macrophage lineage, compared to *H. bilis*-infected *Rag2*$^{-/-}$ mice treated with PBS-coated (placebo) liposomes (Fig. 5). Briefly, the cytokine genes that were transcriptionally suppressed in the clodronate-treated *H. bilis*-infected *Rag2*$^{-/-}$ group included IL-1β (an important proinflammatory mediator produced by activated macrophages, also an inducer of Cox2) ($P < 0.0001$) and TNF-α (a proinflammatory cytokine produced by activated macrophages and involved in systemic inflammatory response) ($P = 0.007$). Also, decreased were IL-10 (an anti-inflammatory cytokine with pleotrophic effects produced by macrophages and lymphocytes) ($P = 0.037$), iNOS (an inducible nitric oxide synthase produced by activated macrophages and epithelial cells and important in innate immune defense against pathogens) ($P = 0.025$), and Cxcl1 (a neutrophil chemoattractant produced by macrophages, neutrophils, and epithelial cells) ($P = 0.0069$). Interestingly, in the *H. bilis*-infected *Rag2*$^{-/-}$ mice that were treated with clodronate, the mRNA levels of various cytokines were suppressed to the extent that these values were not significantly different from those observed with uninfected *Rag2*$^{-/-}$ controls. However, the mRNA levels of the *Cox2* gene in all three different groups were comparable, implying the lack of a direct effect of macrophage depletion on the levels of *Cox2* gene expression in the cecum. A similar comparative analysis of the expression levels of various cytokines was performed on the data obtained from WT mice that were either uninfected (control) or those infected with *H. bilis* and treated with clodronate-encapsulated liposomes or PBS (placebo)-encapsulated liposomes. As expected, given the lack of any pathology in the ceca of all WT mice, there was no difference in the levels of these select gene targets irrespective of infection or clodronate treatment (data not shown).

Colonization levels of *H. bilis* in the cecum of *Rag2*$^{-/-}$ mice is significantly decreased upon macrophage depletion. Interest-

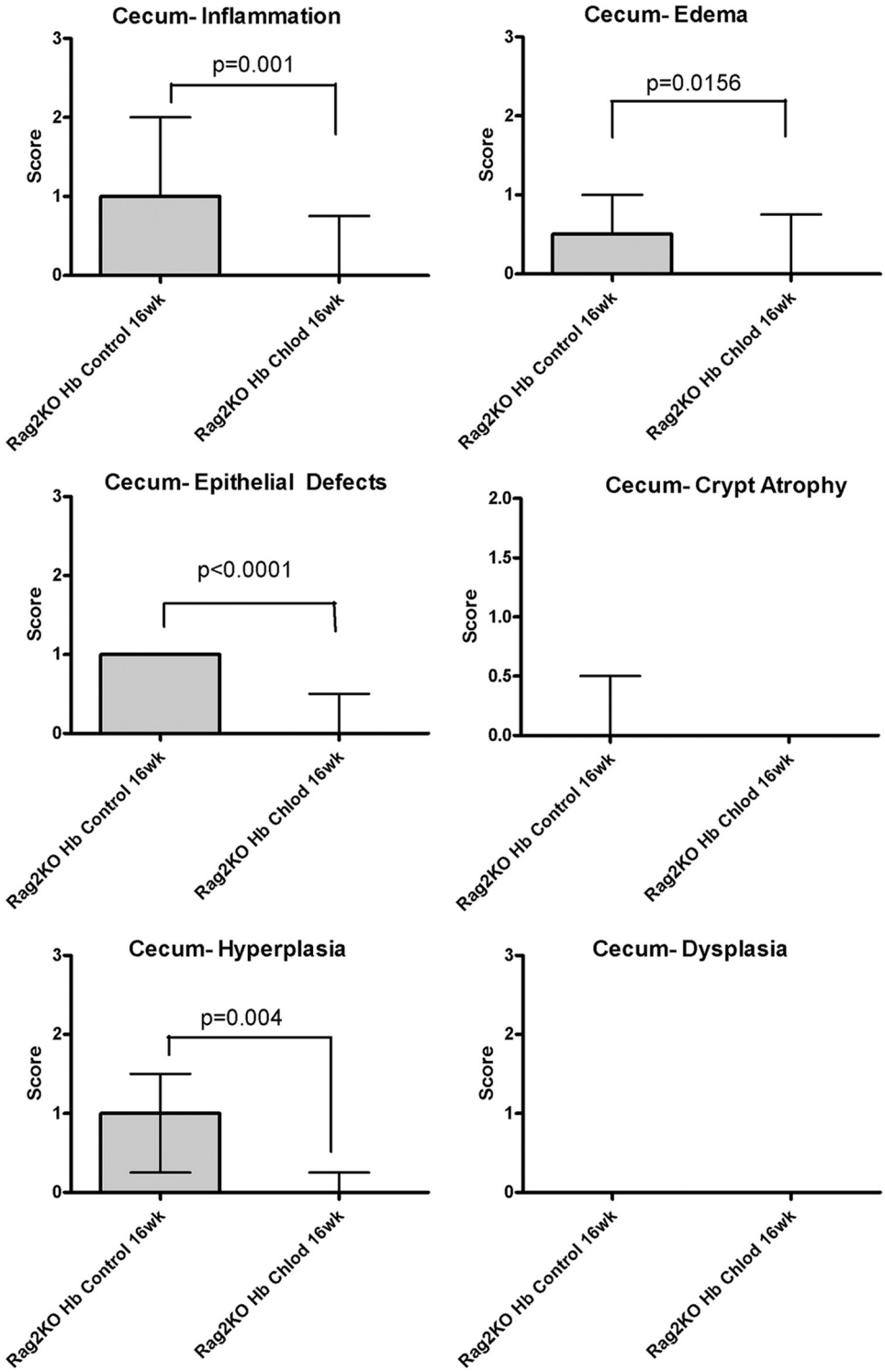

FIG 2 Individual cecal histopathological parameter scores for inflammation, edema, epithelial defects, crypt atrophy, hyperplasia, and dysplasia and cumulative typhlitis index in *H. bilis*-infected *Rag2*$^{-/-}$ (Rag2KO) mice at 16 wpi treated with either clodronate or PBS (placebo)-encapsulated liposomes (7 days posttreatment). Individual bars represent median scores with interquartile ranges, and the *P* values are shown when significant (*, $P < 0.05$; **, $P < 0.01$; ***, $P < 0.001$).

ingly, as shown in the *H. bilis* quantitative PCR data presented in Fig. 6, systemic depletion of macrophages negatively impacted ($P < 0.05$) the colonization ability of *H. bilis* in the *Rag2*$^{-/-}$ mice compared to the PBS (placebo)-treated *Rag2*$^{-/-}$ mice. In the WT mice, there was no discernible effect of macrophage depletion on the levels of *H. bilis* colonization. The levels of colonization in both the macrophage-depleted (clodronate liposome) and the nondepleted (PBS liposome) groups of WT type mice were simi-

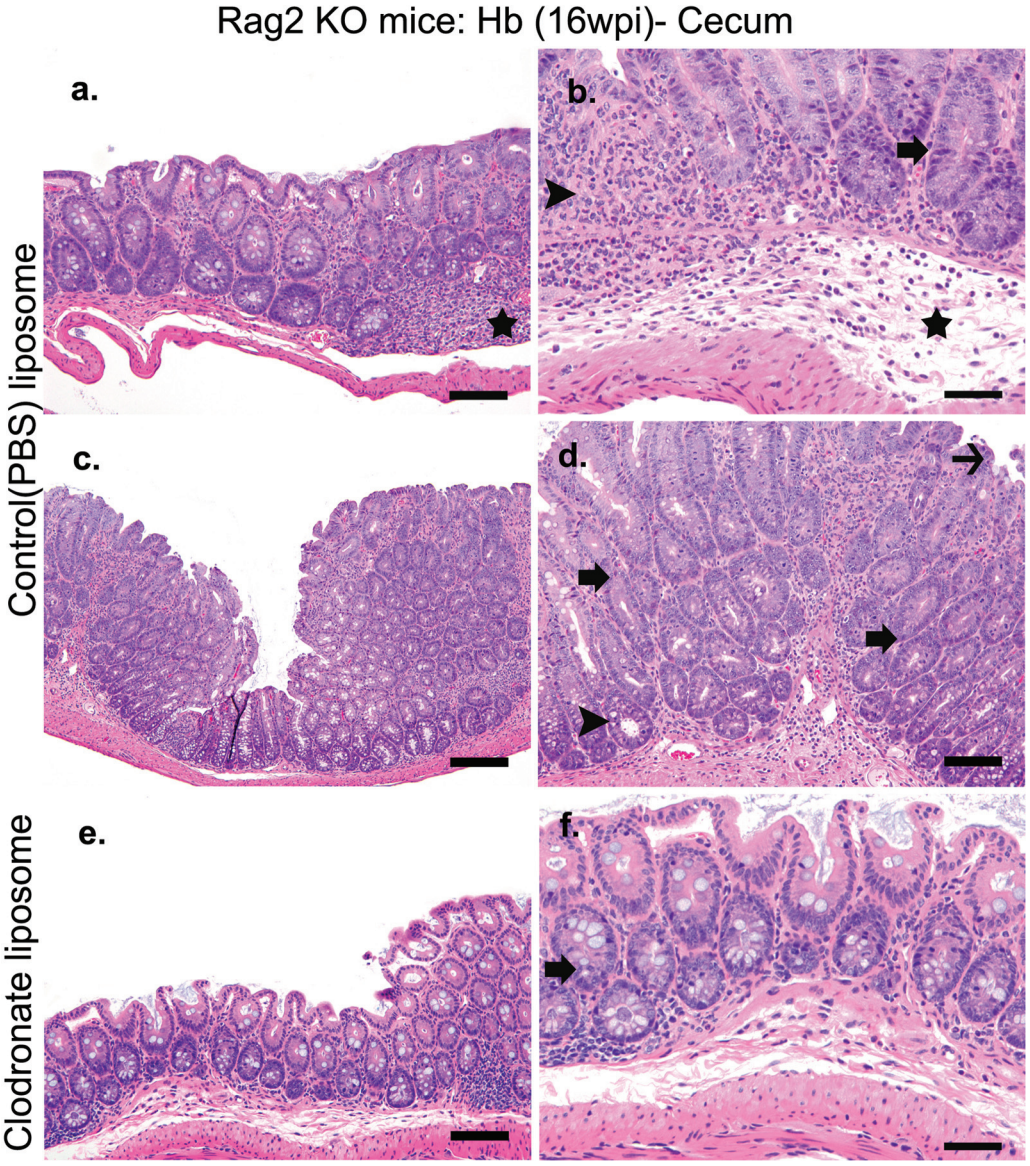

FIG 3 Representative H&E-stained images of the ceca from *H. bilis*-infected *Rag2*$^{-/-}$ (Rag2KO) mice at 16 wpi treated with either control (PBS) liposome (a to d) or clodronate-encapsulated liposomes (e and f). (a) Low-power magnification of the cecum from an *H. bilis*-infected mice treated with PBS liposomes (control) showing mucosal thickening from expansion of lamina propria by inflammatory aggregates (star), mild epithelial hyperplasia, and mucosal vascular congestion. (b) Higher magnification of the cecum from another *H. bilis*-infected control animal showing prominent mucosal and submucosal infiltrates of macrophages and granulocytes (arrowhead), submucosal edema (star), and glandular hyperplasia and loss of normal epithelial mucous (arrow). (c) Low-magnification image of an *H. bilis*-infected control cecum with moderate inflammation, epithelial hyperplasia, and mild epithelial defects. (d) Higher magnification of the image in panel c showing moderate lamina propria expansion by inflammatory cells, mild surface epithelial tethering/loss (thin arrow), occasional mild glandular luminal distension and loss of epithelial mucous (arrowhead), and hyperplastic glandular and surface epithelium with mild architectural disorientation (thick arrows). (e and f) Images showing the ceca of *H. bilis*-infected *Rag2*$^{-/-}$ mice treated with clodronate liposomes at both low-power (e) and high-power (f) magnifications showing a high degree of mucosal recovery and minimal pathology, as characterized by low numbers of inflammatory cells, a high degree of preservation of epithelial mucous, and an absence of significant hyperplasia and other associated changes. Scale bars: a, d, and e, 75 μm; b and f, 40 μm; c, 150 μm.

lar, highlighting that *H. bilis* colonization alone is not sufficient to induce significant typhlocolitis in immunocompetent mice with functional immune systems.

DISCUSSION

The innate immune cells—macrophages, DCs, and neutrophils—are considered to be a prime cellular component of the chronic proinflammatory state of the gut and, during the course of IBD, depletion of macrophages promotes positive therapeutic effects in humans and experimental mice (5, 10, 35, 36, 53). Experimental or therapeutic clinical trials using selective leukocytopharesis or depletion strategies for the depletion of granulocytes and/or monocytes are considered to be safe with various levels of efficacy on mucosal healing (16, 42). In the present study, by utilizing *Rag2*$^{-/-}$ mice that are deficient in functional T and B cells, we analyzed the contribution of innate immune components in a

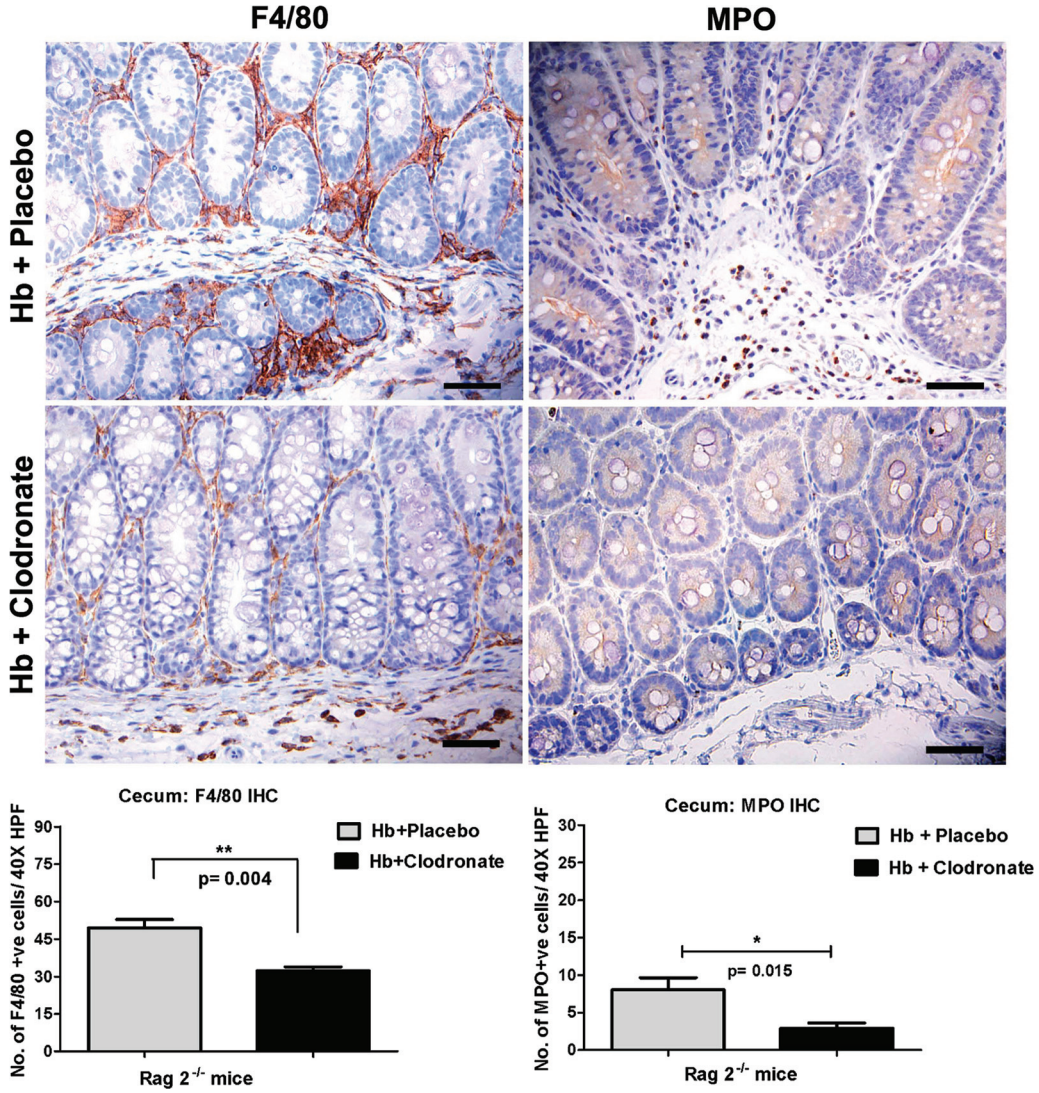

FIG 4 Cecal F4/80$^+$ and MPO$^+$ immunohistochemistry. Five well-oriented ×40 objective microscopic fields from immunostained cecal sections of *H. bilis*-infected *Rag2*$^{-/-}$ mice ($n = 6$ per group) treated with either clodronate or placebo (PBS) were quantitatively assessed for the total numbers of F4/80$^+$ macrophages (top left and middle left panels, respectively) and MPO$^+$ cells (neutrophils chiefly) (top right and middle right panels, respectively) in the mucosa and submucosa. Note the significant reduction in the numbers of positively immunostained (cytoplasmic) macrophages and neutrophils in the ceca of *H. bilis*-infected mice after treatment with clodronate liposomes in the middle panels compared to their respective placebo (PBS)-treated counterparts. Individual bars represent the mean counts ± the SD (*, $P < 0.05$; **, $P < 0.01$; ***, $P < 0.001$). Scale bar, 40 μm.

murine IBD-like state. Our study clearly demonstrates the beneficial effects of a systemic macrophage depletion strategy during the course of *H. bilis*-induced typhlocolitis. These data are also consistent with an earlier study from our laboratory that revealed that macrophages were a major inflammatory cellular component during the course of *H. bilis*-induced typhlocolitis in [Tac:Icr:Ha(ICR)-*scidf*DF] *Scid* mice (46). Cecal cytokine data in the current study showed that *H. bilis* infection in *Rag2*$^{-/-}$ mice by itself enhances the gene expression levels of IL-10, TNF-α, IL-1β, Cxcl1, and iNOS and, correspondingly, depletion of macrophages also simultaneously resulted in a significant reduction of all of these transcripts with an associated decrease in cecal MPO$^+$ cell counts (chiefly neutrophils).

Macrophages may be classified as classically activated macrophages (CAMs or M1), which are important for microbicidal activity, or alternatively activated macrophages (AAMs or M2), that in turn can be further subdivided into wound healing macrophages (for tissue repair) or regulatory macrophages (anti-inflammatory role) (10, 19). CAMs are formed in response to TNF-α and IFN-γ and are associated with Th1-mediated responses, including the secretion of TNF-α, IL-1, IL-6, IL-12, and IL-23, the activation of the Th17 pathway, and the induction of IL-17 and iNOS, a potent chemoattractant for neutrophils (2, 5, 10, 19, 37). Wound-healing macrophages are important in tissue repair and produced in response to stimulation by IL-4 via Th2 helper cell activation or elaborated from basophils/granulocytes following tissue injury or contact with chitin, all of which result in an increased production of collagen and extracellular matrix with a concomitant decrease in tissue iNOS levels (5, 10, 19, 37). Regulatory macrophages are activated in response to various stimuli, including immune com-

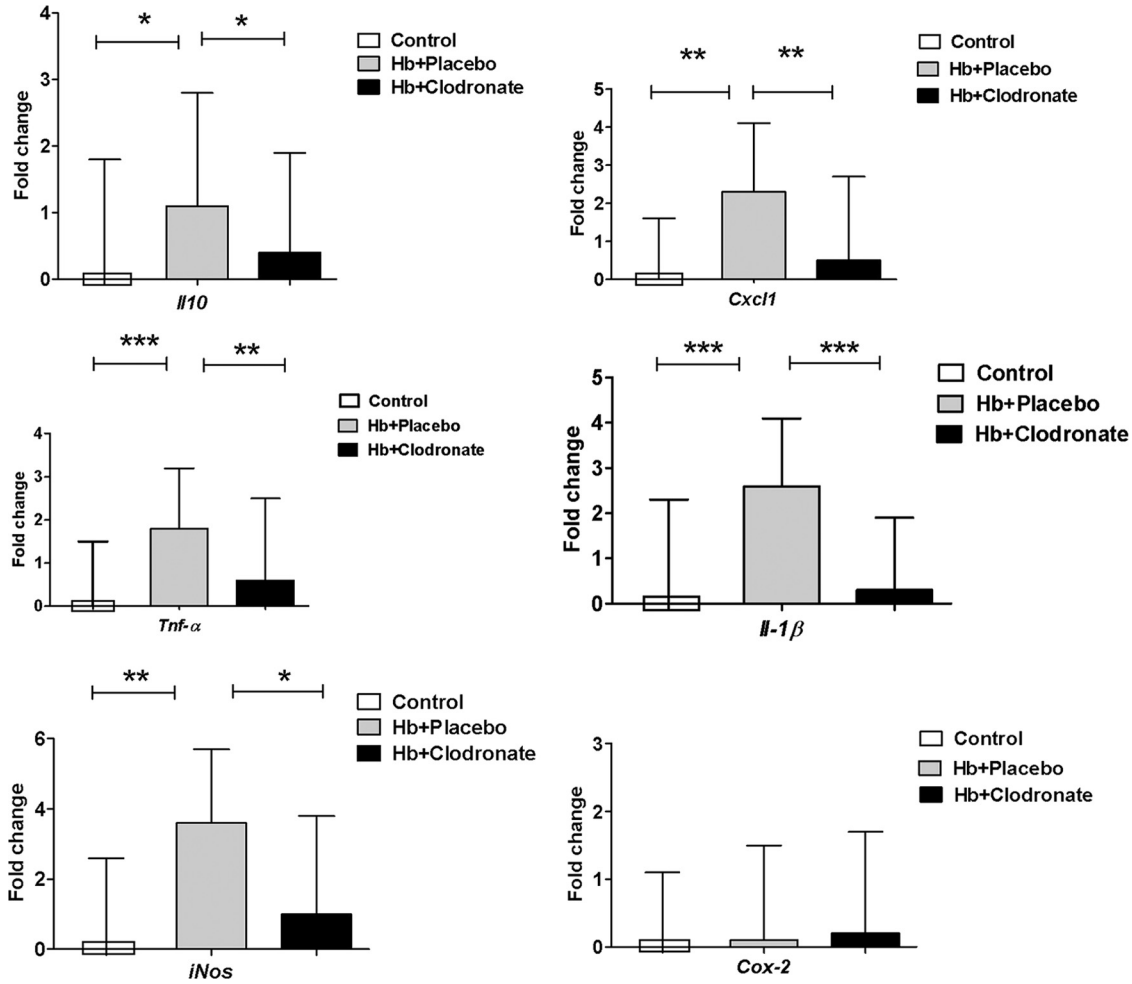

FIG 5 Relative mRNA levels of select inflammatory mediators in the ceca of *Rag2*$^{-/-}$ mice. In each sample, the target gene mRNA was normalized to that of GAPDH. Numbers on the left represent the mean fold change of the individual mRNA levels in reference to the control group (defined as 0, meaning no change). Bars represent the SD. The *P* values for *H. bilis*-infected *Rag2*$^{-/-}$ mice treated with placebo (PBS liposomes, $n = 13$) or clodronate liposomes ($n = 13$) compared to the sham (uninfected *Rag2*$^{-/-}$) controls ($n = 4$) are indicated (*, $P < 0.05$; **, $P < 0.01$; ***, $P < 0.001$).

plexes, prostaglandins, G protein-coupled ligands, glucocorticoids, apoptotic cells, or the anti-inflammatory cytokine IL-10, the result being an increase in IL-10 expression levels and the promotion of Th2 helper T cell responses (2, 10, 19, 40). In a C57BL/6 IL-10$^{-/-}$ mouse model of spontaneous enterocolitis, local macrophage depletion via rectal administration of poly-D,L-lactic acid microspheres containing dichloromethyl diphosphonate (CL_2MDP) attenuated chronic colitis, thus underlying the critical role of resident gut macrophages in the progression of IBD (50). In the context of both commensal and pathogenic gut microflora, certain populations of regulatory anti-inflammatory nonmigratory intestinal macrophages (F4/80$^+$ Cd11b$^+$ Cd11c$^{+/-}$) produce IL-10 in the gut mucosa following recognition and activation by pattern recognition receptors, such as TLRs, TLR agonists, and nucleotide-binding oligomerization domains (NODs) (1, 5, 37). This expression of IL-10 occurs via engagement of $\alpha_v\beta_1$ integrin, a receptor for Sema7A that is expressed on the basolateral aspects of the epithelial cells, and it has been shown that Sema7A-deficient mice are prone to the development of severe DSS-induced colitis due to a concomitant suppression of IL-10 (23).

In this study, on the basis of the increased gene expression

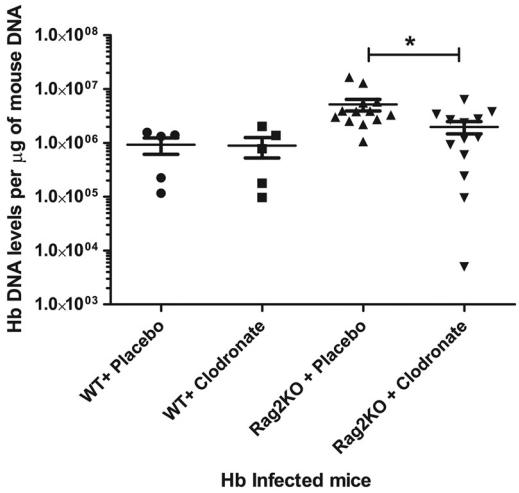

FIG 6 Colonization levels of cecal *H. bilis* estimated by quantitative PCR at 16 wpi. Numbers on the *y* axis represent copy numbers of the *H. bilis* genome per μg of mouse DNA in the corresponding samples. *, $P < 0.05$; **, $P < 0.01$; ***, $P < 0.001$.

levels of TNF-α and IL-1β in association with *H. bilis* colonization in *Rag2*$^{-/-}$ mice, it is assumed that CAMs were the primary activated macrophages during *H. bilis* infection with a concomitant unsuccessful host immune-driven compensatory activation of regulatory macrophages and enhanced IL-10 expression. Clodronate treatment is presumed to have affected all classes of macrophages, as well as DCs, and thus both pro- and anti-inflammatory (IL-10) macrophage-related cytokines mRNA levels were suppressed in the cecum. On a similar note, systemic administration of clodronate-coated liposomes during *H. pylori* infection in a Mongolian gerbil model of gastritis and gastric carcinoma resulted in a net beneficial effect, as demonstrated by a reduction of both infiltrating macrophages and neutrophils with an associated decrease in macrophage activation-related NF-κB-regulated cytokine expression levels in the stomach, although its concomitant effect on bacterial colonization dynamics, if any, was not studied (54). In a recent pertinent study exploiting *H. bilis* adoptive transfer procedures in CD11cTg/*Rag2*$^{-/-}$ mice, it was shown that DCs expressing major histocompatibility complex II alone were sufficient to trigger colitis in the presence of *H. bilis* and T cells (30). Although the precise contribution of DCs was not explored in our study, we believe that these cells also play a role complementary to that of macrophages during *H. bilis*-induced typhlocolitis, and clodronate treatment also affected DCs along with macrophages.

IL-1 is an important proinflammatory mediator in inflammation and autoimmune disease and is produced in two isoforms, IL-1α and IL-1β; IL-1β is secreted by classically activated macrophages and is also an inducer of Cox2 (17). In a TLR5 KO mouse model of colitis, IL-1β was shown to be the primary mediator of proinflammatory immune dysregulation (3). CXCL1 (a neutrophil chemoattractant produced by macrophages, neutrophils, and epithelial cells) was shown to be upregulated during acute DSS-induced colitis in mice, along with other chemokines, such as CXCL2/3, CXCL10, CCL2, CCL4, and CCL22, and an associated downregulation of PGE_2 (31) in a manner similar to that encountered in IBD patients (6). Reactive oxidative and nitrogen species have been long been incriminated as key players in inflammation-driven epithelial and subcellular molecular defects/mutations in both human patients and animal models (2, 7, 21, 26, 33). In a *H. hepaticus*-mediated 129/SvEv *Rag2*$^{-/-}$ mouse model of colitis and colon cancer, it was shown that nitric oxide (NO) and TNF-α trigger colonic inflammation and carcinogenesis and a synthetic iNOS inhibitor prevented NO production, suppressed mucosal pathology, and inhibited carcinogenesis (7). Also, this increased iNOS expression and cancer formation required the presence of Gr-1^{+} neutrophils and an enhanced level of TNF-α expression in the colon, whereas IL-10 downregulated TNF-α and iNOS expression (7). Similarly, TNF-α, NO, and iNOS levels, as well as MPO levels, are frequently elevated in biopsy samples from patients with IBD (2, 21, 33, 48, 53).

A surprising observation in the present study was the negative effect of systemic macrophage depletion on *H. bilis* colonization levels in *Rag2*$^{-/-}$ mice; this finding contrasted with the unaltered *H. bilis* colonization levels in their WT mouse counterparts. In both *Rag2*$^{-/-}$ and WT mice, our macrophage depletion strategy was performed in the context of an established *H. bilis* infection (15 wpi) by which time significant typhlocolitis is observed only in *Rag2*$^{-/-}$ mice. A direct correlation between macrophage numbers (systemic/local) and *H. bilis* colonization density in the immunodeficient setting of *Rag2*$^{-/-}$ mice highlights the importance of both macrophages and bacteria, i.e., *H. bilis*, in the promotion of an inflammatory IBD-like state in this experimental model. Bacterial colonization levels following clodronate liposome-mediated macrophage depletion has not explored in relation to typhlocolitis models in mice, particularly with respect to enteric *Helicobacter* spp. The *in vivo* interaction between macrophages and *H. bilis*, along with a detailed microbial analysis of other gut flora, will be required to determine whether *H. bilis* colonization levels were transient or prolonged after macrophage depletion.

In conclusion, using a *Rag2*$^{-/-}$ mouse model of *H. bilis*-induced typhlocolitis, we have shown that systemic depletion of macrophages imparts a net positive anti-inflammatory effect by amelioration of typhlocolitis with a concomitant reduction in intestinal macrophages and MPO^{+} neutrophils, as well as the suppression of macrophage-related cytokines (IL-1β, IL-10, TNF-α, iNOS, and CXCL1). The data from our study are particularly relevant in the context of understanding the complexity of gut microbe-host immune homeostasis in the pathophysiology of IBD and for developing future novel therapeutic strategies.

ACKNOWLEDGMENTS

This study was supported by National Institutes of Health grants T32 RR007036 (J.G.F.), R01DK052413 (J.G.F.), R01CA067529 (J.G.F.), P01CA026731 (J.G.F.), P30-ES02109 (J.G.F.), and R01R0011141 (J.G.F.).

We thank the MIT DCM Histology Laboratory for its technical assistance.

REFERENCES

1. **Abraham C, Medzhitov R.** 2011. Interactions between the host innate immune system and microbes in inflammatory bowel disease. Gastroenterology **140**:1729–1737.
2. **Beck PL, et al.** 2007. Inducible nitric oxide synthase from bone marrow-derived cells plays a critical role in regulating colonic inflammation. Gastroenterology **132**:1778–1790.
3. **Carvalho FA, et al.** 2012. Interleukin-1β (IL-1β) promotes susceptibility of Toll-like receptor 5 (TLR5)-deficient mice to colitis. Gut **61**:373–384.
4. **Cho JH, Brant SR.** 2011. Recent insights into the genetics of inflammatory bowel disease. Gastroenterology **140**:1704–1712.
5. **Denning TL, Wang YC, Patel SR, Williams IR, Pulendran B.** 2007. Lamina propria macrophages and dendritic cells differentially induce regulatory and interleukin 17-producing T cell responses. Nat. Immunol. **8**:1086–1094.
6. **Egesten A, et al.** 2007. The proinflammatory CXC-chemokines GRO-α/CXCL1 and MIG/CXCL9 are concomitantly expressed in ulcerative colitis and decrease during treatment with topical corticosteroids. Int. J. Colorectal Dis. **22**:1421–1427.
7. **Erdman SE, et al.** 2009. Nitric oxide and TNF-alpha trigger colonic inflammation and carcinogenesis in *Helicobacter hepaticus*-infected, *Rag2*-deficient mice. Proc. Natl. Acad. Sci. U. S. A. **106**:1027–1032.
8. **Eri R, McGuckin MA, Wadley R.** 2012. T cell transfer model of colitis: a great tool to assess the contribution of T cells in chronic intestinal inflammation. Methods Mol. Biol. **844**:261–275.
9. **Ericsson AC, et al.** 2010. Noninvasive detection of inflammation-associated colon cancer in a mouse model. Neoplasia **12**:1054–1065.
10. **Fleming BD, Mosser DM.** 2011. Regulatory macrophages: setting the threshold for therapy. Eur. J. Immunol. **41**:2498–2502.
11. **Fox JG, et al.** 1998. Hepatic *Helicobacter* species identified in bile and gallbladder tissue from Chileans with chronic cholecystitis. Gastroenterology **114**:755–763.
12. **Fox JG, Ge Z, Whary MT, Erdman SE, Horwitz BH.** 2011. *Helicobacter hepaticus* infection in mice: models for understanding lower bowel inflammation and cancer. Mucosal Immunol. **4**:22–30.
13. **Fox JG, et al.** 2004. *Helicobacter bilis*-associated hepatitis in outbred mice. Comp. Med. **54**:571–577.
14. **Fox JG, et al.** 2009. Chronic hepatitis, hepatic dysplasia, fibrosis, and biliary hyperplasia in hamsters naturally infected with a novel *Helicobacter* classified in the *H. bilis* cluster. J. Clin. Microbiol. **47**:3673–3681.

15. **Fox JG, et al.** 1995. *Helicobacter bilis* sp. nov., a novel *Helicobacter* species isolated from bile, livers, and intestines of aged, inbred mice. J. Clin. Microbiol. **33**:445–454.
16. **Fukuchi T, et al.** 2011. Rapid induction of mucosal healing by intensive granulocyte and monocyte adsorptive aphaeresis in active ulcerative colitis patients without concomitant corticosteroid therapy. Aliment. Pharmacol. Ther. **34**:583–585.
17. **Gabay C, Lamacchia C, Palmer G.** 2010. IL-1 pathways in inflammation and human diseases. Nat. Rev. Rheumatol. **6**:232–241.
18. **Ge Z, et al.** 2011. Coinfection with Enterohepatic *Helicobacter* species can ameliorate or promote *Helicobacter pylori*-induced gastric pathology in C57BL/6 mice. Infect. Immun. **79**:3861–3871.
19. **Gordon S, Martinez FO.** 2010. Alternative activation of macrophages: mechanism and functions. Immunity **32**:593–604.
20. **Haines DC, et al.** 1998. Inflammatory large bowel disease in immunodeficient rats naturally and experimentally infected with *Helicobacter bilis*. Vet. Pathol. **35**:202–208.
21. **Hartnett L, Egan LJ.** 2012. Inflammation, DNA methylation, and colitis-associated cancer. Carcinogenesis **33**:723–731.
22. **Horwitz BH.** 2007. The straw that stirs the drink: insight into the pathogenesis of inflammatory bowel disease revealed through the study of microflora-induced inflammation in genetically modified mice. Inflamm. Bowel Dis. **13**:490–500.
23. **Kang S, et al.** 2012. Intestinal epithelial cell-derived semaphorin 7A negatively regulates development of colitis via αvβ1 integrin. J. Immunol. **188**:1108–1116.
24. **Kosaka T, et al.** 2010. *Helicobacter bilis* colonization of the biliary system in patients with pancreaticobiliary maljunction. Br. J. Surg. **97**:544–549.
25. **Lehenkari PP, et al.** 2002. Further insight into mechanism of action of clodronate: inhibition of mitochondrial ADP/ATP translocase by a non-hydrolyzable, adenine-containing metabolite. Mol. Pharmacol. **61**:1255–1262.
26. **Lemke LB, et al.** 2009. Concurrent *Helicobacter bilis* infection in C57BL/6 mice attenuates proinflammatory *H. pylori*-induced gastric pathology. Infect. Immun. **77**:2147–2158.
27. **Liu Z, et al.** 2009. Mucosal gene expression profiles following the colonization of immunocompetent defined-flora C3H mice with *Helicobacter bilis*: a prelude to typhlocolitis. Microbes Infect. **11**:374–383.
28. **Liu Z, et al.** 2011. *Helicobacter bilis* colonization enhances susceptibility to typhlocolitis following an inflammatory trigger. Dig. Dis. Sci. **56**:2838–2848.
29. **Maggio-Price L, et al.** 2005. Dual infection with *Helicobacter bilis* and *Helicobacter hepaticus* in P-glycoprotein-deficient *Mdr1a*$^{-/-}$ mice results in colitis that progresses to dysplasia. Am. J. Pathol. **166**:1793–1806.
30. **Maggio-Price L, et al.** 22 May 2012. Lineage targeted MHC-II transgenic mice demonstrate the role of dendritic cells in bacterial-driven colitis. Inflamm. Bowel Dis. [Epub ahead of print.] doi:10.1002/ibd.23000.
31. **Melgar S, Drmotova M, Rehnstrom E, Jansson L, Michaelsson E.** 2006. Local production of chemokines and prostaglandin E_2 in the acute, chronic, and recovery phase of murine experimental colitis. Cytokine **35**:275–283.
32. **Nell S, Suerbaum S, Josenhans C.** 2010. The impact of the microbiota on the pathogenesis of IBD: lessons from mouse infection models. Nat. Rev. Microbiol. **8**:564–577.
33. **Pavlick KP, et al.** 2002. Role of reactive metabolites of oxygen and nitrogen in inflammatory bowel disease. Free Radic. Biol. Med. **33**:311–322.
34. **Pisani P, et al.** 2008. Cross-reactivity between immune responses to *Helicobacter bilis* and *Helicobacter pylori* in a population in Thailand at high risk of developing cholangiocarcinoma. Clin. Vaccine Immunol. **15**:1363–1368.
35. **Qualls JE, Kaplan AM, van Rooijen N, Cohen DA.** 2006. Suppression of experimental colitis by intestinal mononuclear phagocytes. J. Leukoc. Biol. **80**:802–815.
36. **Qualls JE, Tuna H, Kaplan AM, Cohen DA.** 2009. Suppression of experimental colitis in mice by $CD11c^+$ dendritic cells. Inflamm. Bowel Dis. **15**:236–247.
37. **Rivollier A, He J, Kole A, Valatas V, Kelsall BL.** 2012. Inflammation switches the differentiation program of Ly6Chi monocytes from anti-inflammatory macrophages to inflammatory dendritic cells in the colon. J. Exp. Med. **209**:139–155.
38. **Rizzo A, Pallone F, Monteleone G, Fantini MC.** 2011. Intestinal inflammation and colorectal cancer: a double-edged sword? World J. Gastroenterol. **17**:3092–3100.
39. **Rogers AB, Houghton J.** 2009. *Helicobacter*-based mouse models of digestive system carcinogenesis. Methods Mol. Biol. **511**:267–295.
40. **Rutella S, Locatelli F.** 2011. Intestinal dendritic cells in the pathogenesis of inflammatory bowel disease. World J. Gastroenterol. **17**:3761–3775.
41. **Sanchez-Munoz F, Dominguez-Lopez A, Yamamoto-Furusho JK.** 2008. Role of cytokines in inflammatory bowel disease. World J. Gastroenterol. **14**:4280–4288.
42. **Saniabadi AR, et al.** 2007. Therapeutic leukocytapheresis for inflammatory bowel disease. Transfus. Apher. Sci. **37**:191–200.
43. **Sheh A, et al.** 2011. 17β-estradiol and tamoxifen prevent gastric cancer by modulating leukocyte recruitment and oncogenic pathways in *Helicobacter pylori*-infected INS-GAS male mice. Cancer Prev. Res. (Philadelphia) **4**:1426–1435.
44. **Shen Z, Feng Y, Fox JG.** 2000. Identification of enterohepatic *Helicobacter* species by restriction fragment-length polymorphism analysis of the 16S rRNA gene. Helicobacter **5**:121–128.
45. **Shomer NH, Dangler CA, Marini RP, Fox JG.** 1998. *Helicobacter bilis*/*Helicobacter rodentium* coinfection associated with diarrhea in a colony of scid mice. Lab. Anim. Sci. **48**:455–459.
46. **Shomer NH, Dangler CA, Schrenzel MD, Fox JG.** 1997. *Helicobacter bilis*-induced inflammatory bowel disease in scid mice with defined flora. Infect. Immun. **65**:4858–4864.
47. **Taylor NS, Xu S, Nambiar P, Dewhirst FE, Fox JG.** 2007. Enterohepatic *Helicobacter* species are prevalent in mice from commercial and academic institutions in Asia, Europe, and North America. J. Clin. Microbiol. **45**:2166–2172.
48. **van der Veen BS, de Winther MP, Heeringa P.** 2009. Myeloperoxidase: molecular mechanisms of action and their relevance to human health and disease. Antioxid. Redox Signal. **11**:2899–2937.
49. **Van Rooijen N, Sanders A.** 1994. Liposome-mediated depletion of macrophages: mechanism of action, preparation of liposomes and applications. J. Immunol. Methods **174**:83–93.
50. **Watanabe N, et al.** 2003. Elimination of local macrophages in intestine prevents chronic colitis in interleukin-10-deficient mice. Dig. Dis. Sci. **48**:408–414.
51. **Weisser SB, et al.** 2011. SHIP-deficient, alternatively activated macrophages protect mice during DSS-induced colitis. J. Leukoc. Biol. **90**:483–492.
52. **Weisser SB, van Rooijen N, Sly LM.** 2012. Depletion and reconstitution of macrophages in mice. J. Vis. Exp. **66**:e4105. doi:10.3791/4105.
53. **Xavier RJ, Podolsky DK.** 2007. Unraveling the pathogenesis of inflammatory bowel disease. Nature **448**:427–434.
54. **Yanai A, et al.** 2008. Activation of IκB kinase and NF-κB is essential for *Helicobacter pylori*-induced chronic gastritis in Mongolian gerbils. Infect. Immun. **76**:781–787.